Emerging Polymer-Stabilized Blue Phase Liquid Crystal Display

Jin Yan, Hui-Cheng Cheng, Linghui Rao, Takahiro Ishinabe and Shin-Tson Wu

College of Optics and Photonics, University of Central Florida, Orlando, FL 32816, USA

ABSTRACT

Polymer-stabilized blue-phase liquid crystals hold great potential for future display applications. Some technical challenges, such as blue-phase temperature range, operation voltage, hysteresis, and voltage holding ratio remain to be overcome before widespread commercialization can be realized. In this paper, we review recent advances in this emerging technology.

Keywords: Blue phase, liquid crystal, hysteresis

1. INTRODUCTION

Blue phase liquid crystal (BPLC) has been known for decades, but the narrow temperature range (~0.5-2K) limits its application. In 2002, Kikuchi et al [1] reported a non-reactive BPLC stabilized by a small fraction of polymer (~8 wt%). The cross-linked polymer network is selectively concentrated in the disclination cores and the lattice structure of the blue phase is stabilized. As a result, the temperature range of BPLC is extended to more than 60K, including room temperature (260-326K). This polymer stabilized blue phase has potential to become next-generation display technology due to several attractive features, such as submillisecond gray-to-gray response time, intrinsic wide viewing angle, no need for surface alignment layer, and cell gap insensitivity for in-plane switching (IPS) mode. Especially, the fast response time of BPLC composite enables color sequential displays using RGB LEDs, which in turn eliminates the spatial color filters. Consequentially, the optical efficiency and resolution density are all tripled. However, several technical challenges, such as relatively narrow temperature range, relatively high operating voltage, hysteresis, stability, contrast ratio, and low voltage holding ratio remain to be overcome before widespread application can be realized.

In this paper, we review recent progresses on this emerging display technology, including materials and device structures. Each of key performance factors will be analyzed and possible solutions discussed.

2. BLUE PHASE MATERIALS

Blue phases are mesophases that appear over a narrow temperature range between chiral nematic and isotropic phases. Polymer stabilization method greatly widens the blue phase temperature range, but is still relatively narrow. For display applications, the LC temperature range should cover from -40 °C to 80 °C. A polymer-stabilized BPLC consists of LC host, chiral dopant and polymers. At first, we could choose a wide temperature range nematic LC host. However, after mixing with chiral dopant the mixture's clearing point often decreases substantially. For example, the clearing temperature of a LC host is 94ºC, but it drops to 54ºC after polymerization. This is because the employed chiral dopant has a very low clearing point. A low clearing point PSBP will make the electro-optic properties of the

LC/polymer composite, e.g., VT curves and response time too sensitive to the local temperature variation of a display panel. Consequently, the requirement for better thermal uniformity of a backlight unit is increased. To avoid the dramatic decrease of clearing temperature, a chiral dopant with high twisting power and high melting point would help. Meanwhile, its solubility should also be taken into consideration.

Macroscopically, a polymer-stabilized BPLC is optically isotropic. When a small electric field (E) is applied to a PS-BPLC composite, the LC molecules tend to be reoriented parallel to the electric field if $\Delta\varepsilon > 0$, and perpendicular to the electric field if $\Delta\varepsilon < 0$, where $\Delta\varepsilon$ is the dielectric anisotropy of the LC. Such molecular reorientation results in a birefringence in BPLC and the induced birefringence can be described by Kerr effect as:

$$\Delta n_{ind} = \lambda K E^2 \tag{1}$$

where λ is the wavelength and K is the Kerr constant [2]. BPLC has a fairly large Kerr constant compared to conventional isotropic Kerr medium, due to the short range interaction between liquid crystal molecules. The Kerr constant of BPLC was determined by several LC parameters as [3]:

$$K \approx \Delta n \cdot \Delta\varepsilon \frac{\varepsilon_o P^2}{k\lambda(2\pi)^2} \tag{2}$$

where Δn, $\Delta\varepsilon$, and k are the intrinsic birefringence, dielectric anisotropy, and elastic constant of the host LC material, and P is the pitch length. A large Kerr constant helps to reduce the driving voltage of BP LCD. From Eq. (2), to enhance Kerr constant, a liquid crystal with large Δn and large $\Delta\varepsilon$ should be employed. For example, Chisso JC-BP01M has a large Kerr constant ~13.7 nm/V^2 because its host LC has $\Delta n \sim 0.17$ and $\Delta\varepsilon \sim 94$ [4]. Meanwhile, the clearing temperature of Chisso JC-BP01M is ~70°C.

From Eq. (2), pitch length also plays an important role affecting Kerr constant. Normally, to make a transparent blue-phase LCD, a short pitch length is needed so that its corresponding Bragg reflection occurs at ~350 nm. A strategy to enhance Kerr constant is to increase pitch length, i.e., to shift the reflection band of the blue phase to near infrared region (~750 nm) and use surface treatment method to eliminate the higher order reflection bands in the visible region.

3. LOW VOLTAGE DEVICES

Enhancing Kerr constant by increasing the $\Delta n \cdot \Delta\varepsilon / k$ of host LC will unavoidably lead to increased viscosity, which in turn lengthens the response time. Optimizing the device structure is an effective way to reduce the operating voltage [5, 6]. For instance, using Chisso JC-BP01M in an IPS cell with 10-μm electrode width and 10-μm electrode gap, the driving voltage is ~50V. In 2009, Rao et al. proposed protrusion electrodes to generate strong horizontal electric field which penetrates deeply into the bulk liquid crystal layer [7]. By optimizing the electrode dimensions, the on-

state voltage could be reduced to ~10V and the corresponding transmittance is ~70%. In 2010, Jiao et al. proposed a corrugated structure to produce uniform electric field and two domains [8]. This electric field has strong horizontal component and more importantly, the field penetrates into the whole LC medium. This design not only reduces the voltage to ~10V but also increases the transmittance to ~85%. The major advantages of these lateral field approaches are twofold: 1) wide view can be easily achieved by using only one biaxial film, and 2) the VT curves are fairly insensitive to the cell gap for the protrusion structure, as long as the cell gap exceeds the field's penetration depth. However, the major shortcoming of these protruded electrode structures is the increased fabrication complexity.

To overcome the fabrication problem, in 2011 a vertical field switching (VFS) mode was proposed independently by Cheng et al [9] and Kim et al [10]. In Ref. [10], the normally incident backlight is split into oblique rays by a prism array before impinging the BPLC cell. The device structure is fairly simple, but two problems remain to be overcome: double images and low optical efficiency because some of the light cannot pass through the prisms. Moreover, the light propagation angle inside the BPLC cell is relatively small. While in Ref. [9], the incident light is set at ~70° so that the operating voltage is greatly reduced and hysteresis is completely suppressed. By using a thin cell gap, the operating voltage could be reduced to ~10V while eliminating the hysteresis. Moreover, the transmittance (normalized to that of two parallel polarizers) can reach 100% because there is no dead zone. The uniform electric field also helps to reduce response time.

Figure 1 depicts the proposed VFS BPLC device structure. Because the electric field is in the longitudinal direction, only the incident light at an oblique angle can experience the phase retardation effect. For a given BPLC layer thickness, a larger incident angle results in a larger phase retardation, which helps to lower the operating voltage. Therefore, we need to couple the backlight to a large output angle (e.g., $\theta \sim 70°$) and keep it reasonably well collimated.

The bottom coupling film laminated on the bottom polarizer can substantially couple the oblique incident light to the bottom substrate and the BPLC layer. It has a prismatic structure which not only couples the oblique input light to the cell but also keeps a large angle. The function of the top coupling film is to couple the light to the air. Without this top coupling film, the oblique angle light will be trapped in the cell module because of total internal reflection (TIR). Placed on the top coupling film, the turning film can steer the direction of the oblique light to the viewer's position by TIR. To widen viewing angle, a forward diffuser which has negligible reflection to the ambient light could be employed.
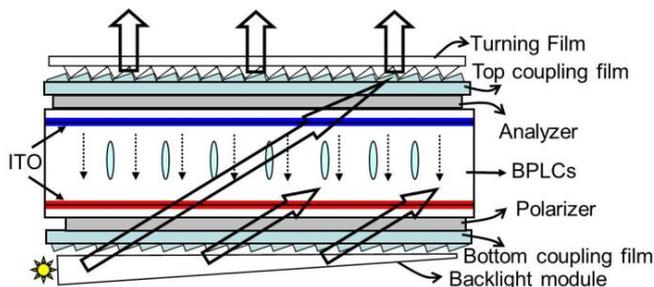

Figure 1. Device structure of the proposed VFS blue-phase LCD.

To confirm the advantages of our VFS device over the conventional IPS structure, we performed some experiments. Figure 2 shows the experimental setup for our VFS cell. To simulate function of the coupling film, we prepared a transparent box filled with Glycerol (n=1.47@ λ=633 nm). The cell was immersed in the Glycerol liquid and it can be oriented at an arbitrary angle. Because Glycerol has a much larger index than air, the light can pass through the BPLC in a very large angle. To make a fair comparison, we used the same material for both IPS and VFS cells. The IPS cell has patterned ITO electrodes with 10 μm electrode width and 10 μm electrode gap, and the cell gap is $d \sim 7.5$ μm. In the VFS cells, both top and bottom glass substrates were coated with a thin (~80 nm) ITO electrode; no polyimide layer was used. The cell gap was controlled at $d \sim 5.74$ μm.
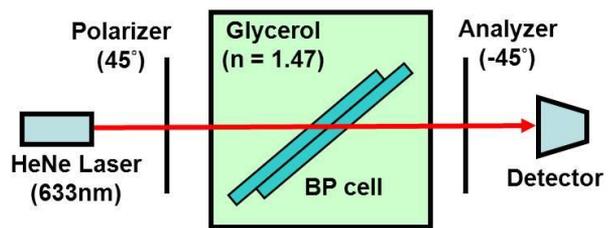

Figure 2. Experimental setup for characterizing the VFS cell.

Figure 3 depicts the measured voltage-dependent transmittance (VT) curves (at λ=633 nm and T~23°C) of the IPS cell and VFS cell at $\theta = 70°$. For the IPS cell measured at normal incidence, the peak voltage occurs at $V_p \sim 50$ V. For the VFS cell at $\theta = 70°$, its $V_p \sim 16$ V which is ~3.2X lower than that of IPS structure. To further reduce operating voltage, we could use a thinner cell gap or increase the incident angle.
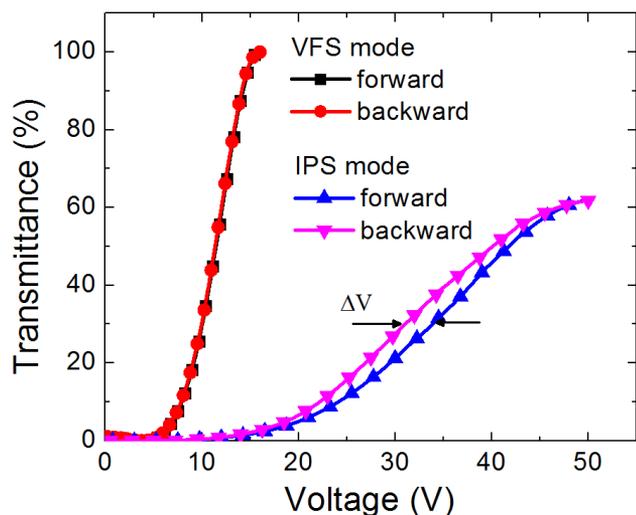

Figure 3. Measured VT curves and hysteresis of IPS and VFS cells. λ=633 nm.

Another drastic difference observed in Fig. 3 is that the IPS cell exhibits a ~5.8% hysteresis, but the VFS cell is free from hysteresis! The reason is that the VFS cell has a fairly low operating voltage (<16V) so that the electrostriction effect does not occur. In an IPS cell, the generated electric fields are not uniform spatially. The electric fields are much stronger near the pixel edges than those in the electrode gap. The strong electric fields could cause lattice deformation locally which in turn contributes to the hysteresis. Hysteresis will be discussed in details in next section.

We also compared the response time of VFS cell and IPS cell. The applied voltage swings from 0 to 16V for the VFS cell, and 0 to 50V for the IPS cell. The measured [rise time, decay time] for the IPS cell and VFS cell are [648 µs, 1795 µs], and [730 µs, 870 µs], respectively. VFS mode shows a ~2X faster decay time than IPS. This is attributed to the smaller LC reorientation angle and uniform field of the VFS cell.

Compared with protrusion and corrugated structures, VFS mode has several merits, such as simple fabrication, high transmittance, hysteresis-free and fast response time. The major challenge for the VFS mode is to achieve wide viewing angle, because the backlight's incident angle is fairly large and has a fairly narrow FWHM. Therefore, this design is suitable for narrow-view applications. To widen the viewing angle, we can design irregular prism structure of turning film to orient backlight to multiple directions or use a front diffuser to spread light more uniformly.

4. HYSTERESIS

Hysteresis affects gray scale control accuracy and needs to be suppressed [11]. In Fig. 3, it was noticed that hysteresis is related to the maximum electric field. Similar phenomenon was also found in IPS cells with different dimensions [12-13]. A stronger electric field induces a larger hysteresis. In Table I, three BPLC samples with different IPS electrode width (*w*) and gap (*l*): 10-10, 5-5, and 2-4 (unit: µm) was compared. A smaller electrode dimension helps to reduce the driving voltage; however, the peak electric field is also stronger. Therefore, the corresponding hysteresis is larger.

Table I: Measured V_{on} and hysteresis, and calculated E_p of IPS test cells at 25°C.

IPS Cell	V_{on} (V)	Hysteresis	E_p at V_{on} (V/µm)
10-10	56.7	6.4%	9.65
5-5	50.7	10.1%	17.53
2-4	40.0	10.0%	16.95

To further investigate the correlation between electric field and hysteresis, we scanned the VT curves to different gray scales for the 10-10 IPS cell, as shown in Fig. 4. When the voltage is high, the hysteresis is evident. However, if we limited the voltage to 28.6V, hysteresis is vanished. The corresponding peak electric field is ~4.9V/µm, which we call the critical field for eliminating hysteresis.

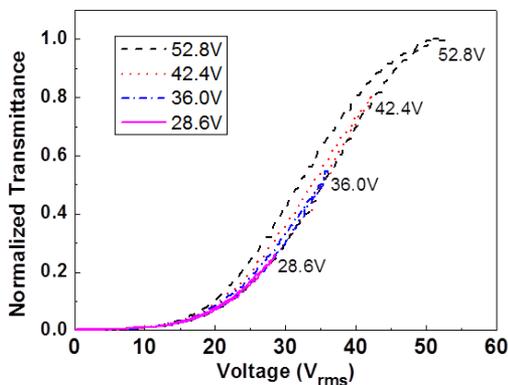Figure 4. Measured hysteresis of the 10-10 IPS cell. PS-BPLC: Chisso JC-BP01M. λ=633 nm.

For a given BPLC material, its peak electric field is strongly related to the device structure. Once the critical field is determined, we should design a device structure whose peak transmittance occurs when the corresponding maximum electric field is below critical field in order to eliminate hysteresis. We have calculated the peak electric field for some IPS and protrusion electrodes. Results are listed in Table II. From Table II, the peak electric field is reduced from 8.65 V/µm for the trapezoid protrusion to 6.85 V/µm for the elliptical protrusion. If the height of the elliptical shape electrode is increased to 4 µm, the peak field is further reduced to ~5 V/µm. With such a low peak electric field, the device would be free from hysteresis.

Table II: Simulated electric field components and peak electric field for some BPLC cell configurations.

Cell	V_{on} (V)	$E_{x\,max}$ (V/µm)	$E_{z\,max}$ (V/µm)	E_p (V/µm)
2-4 IPS (d=7µm)	40	15.53	12.91	16.95
2-4 trapezoid (d=10µm, h=2µm)	17	7.68	3.97	8.65
2-4 elliptical (d=10µm, h=2µm)	18	6.84	6.09	6.85
2-4 elliptical (d=10µm, h=4µm)	13	5.08	5.00	5.08

5. LONG-TERM STABILITY

Long term stability is a crucial issue for all PS-BPLC devices for practical applications. The stability can be characterized in two aspects: residual birefringence and electro-optic performance.

When a strong electric field is applied to a PS-BPLC, the blue phase structure could be distorted and light leakage observed. The latter is called residual birefringence. Residual birefringence degrades the contrast ratio and should be suppressed. We have studied the relation between residual birefringence and polymer concentration [14]. A PS-BPLC requires two kinds of monomers: mono-functional and di-functional monomers. We control the overall monomers concentration, as well as the ratio between the two monomers. As the polymer concentration increases, the residual birefringence is reduced, which indicates the polymer network structure is more stable. Monomer ratio is also important in terms of residual birefringence. For example, we used two kinds of monomers: RM257 and C12A and we chose three weight ratios between the two monomers: 1:1, 2:1, and 3:1. The 1:1 ratio samples exhibit the smallest residual birefringence. Therefore, residual birefringence can be suppressed by optimizing the polymers.

We have also investigated the long-term stability of an IPS cell with Chisso JC-BP01M. To evaluate the long-term stability, the sample was baked in an oven at 70°C. Figures 5 and 6 show the baking time dependent on-state voltage and response time. The measurements were conducted at room temperature (~23°C) with 100 Hz driving frequency. Here the VT curves were measured under crossed polarizers. Overall speaking, both on-state voltage and response time do not change noticeably within one month of baking. The fluctuation of the response time is within 20%.
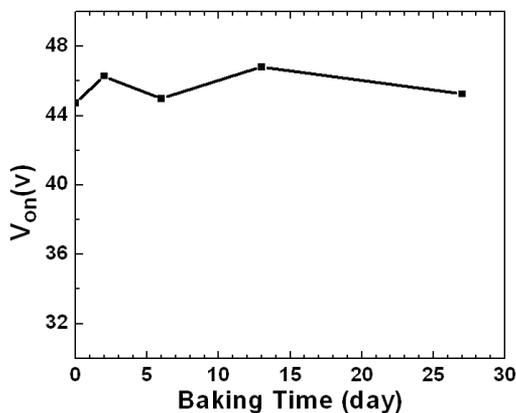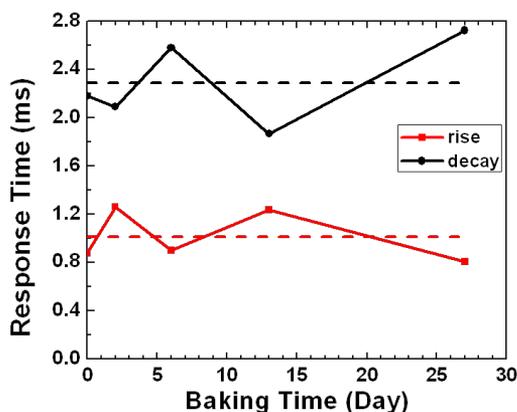
Figure 5. Baking time dependent on-state voltage.

Figure 6. Baking time dependent response time. The dashed lines are averaged rise and decay time.

6. REMAINING CHALLENGES

Besides the abovementioned features, there are some other challenges that need to be taken into consideration.

High contrast ratio is an important criterion for LCDs. There are several factors that can affect the contrast ratio. For example, the defects inside the BPLC cells during the fabrication process could cause light leakage and degrade the contrast ratio. The residual birefringence can also reduce contrast ratio. Some efforts are being conducted to improve the contrast ratio [15].

For TFT-LCD applications, the voltage holding ratio is another crucial requirement in order to avoid image sticking. In a polymer-stabilized BPLC, two types of monomers and a small percentage of photo-initiator are used. The ionic impurities in these monomers and photo-initiator could degrade the voltage holding ratio. Therefore, better materials including LC host, monomers, and photo-initiator need to be developed, and the photo-polymerization process needs to be optimized. Moreover, the residual DC voltage is roughly proportional to the operation voltage. A high operation voltage would increase the level of residual DC voltage and image sticking. Therefore, low voltage BPLC devices are highly desirable from all the performance aspects.

7. CONCLUSION

Tremendous progresses have been made in the past few years. New BPLC materials have been developed to widen the blue phase temperature range and lower the driving voltage to ~50V. Different device structures have been proposed to further reduce the voltage to ~10V and eliminate the hysteresis so that the amorphous silicon TFT addressing was enabled. Polymer concentration and composition effect was also investigated in order to stabilize the blue phase structure. The existing technical issues are being addressed gradually but they remain to be further improved. A big wave of next generation display is emerging.

REFERENCES

1. H. Kikuchi, M. Yokota, Y. Hisakado, H. Yang, and T. Kajiyama, "Polymer-stabilized liquid crystal blue phases," Nat. Mater. **1**, 64-68 (2002).
2. J. Kerr, "A new relation between electricity and light: Dielectrified media birefringent," Philos. Mag. **50**, 337-348 (1875).
3. P. R. Gerber, "Electro-optical effects of a small-pitch blue-phase system," Mol. Cryst. Liq. Cryst. **116**, 197-206 (1985).
4. L. Rao, J. Yan, S. T. Wu, S. Yamamoto, and Y. Haseba, "A large Kerr constant polymer-stabilized blue phase liquid crystal," Appl. Phys. Lett. **98**, 081109 (2011).
5. Z. Ge, S. Gauza, M. Jiao, H. Xianyu, and S. T. Wu, "Electro-optics of polymer-stabilized blue phase liquid crystal displays", Appl. Phys. Lett. **94**, 101104 (2009).
6. Z. Ge, L. Rao, S. Gauza, and S. T. Wu, "Modeling of blue phase liquid crystal displays", J. Display Technol. **5**, 250-256 (2009).
7. L. Rao, Z. Ge, and S. T. Wu, "Low voltage blue-phase liquid crystal displays", Appl. Phys. Lett. **95**, 231101 (2009).
8. M. Jiao, Y. Li, and S. T. Wu, "Low voltage and high transmittance blue-phase liquid crystal displays with corrugated electrodes," Appl. Phys. Lett. 96, 011102 (2010).
9. H. C. Cheng, J. Yan, T. Ishinabe, and S. T. Wu, "Vertical field switching for blue-phase liquid crystal devices," Appl. Phys. Lett. **98**, 261102 (2011).
10. Y. H. Kim, S. T. Hur, K. W. Park, D. H. Park, S. W. Choi, and H. R. Kim, "A vertical-field-driven polymer-stabilized blue phase liquid crystal displays," SID Symposium Digest, **42**, 298-301 (2011).
11. K. M. Chen, S. Gauza, H. Xianyu, and S. T. Wu, "Hysteresis effects in blue-phase liquid crystals," J. Display Technol. **6**, 318-322 (2010).
12. K. M. Chen, J. Yan, S. T. Wu, Y. P. Chang, C. C. Tsai, and J. W. Shiu, "Electrode dimension effects on blue-phase liquid crystal displays," J. Display Technol. **7**, 362-364 (2011).
13. L. Rao, J. Yan, S. T. Wu, Y. H. Chiu, H. Y. Chen, C. C. Liang, C. M. Wu, P. J. Hsieh, S. H. Liu, and K. L. Cheng, "Critical field for a hysteresis-free blue-phase liquid crystal device," J. Display Technol. **7**, (Accepted, 2011).
14. J. Yan and S. T. Wu, "Effect of polymer concentration and composition on blue-phase liquid crystals," J. Display Technol. **7**, 490-493 (2011).
15. D. Kubota, et al., "A new process for manufacture of low voltage, polymer-stabilized blue phase LCDs", SID Symposium Digest **42**, 125-128 (2011).